Pergamon
www.elsevier.com/locate/jappmathmech
PII: S0021-8928(99)00009-X
J. Appl. Maths Mechs, Vol. 63, No. 1, pp. 55–62, 1999

0021-8928/99/$—see front matter

THE INVISCID NATURE OF THE ASYMMETRY OF THE SEPARATING FLOW OF A UNIFORM STREAM AROUND SYMMETRIC BODIES†

A. N. KRAIKO and K. S. REYENT

Moscow

(*Received* 14 *May* 1998)

The "inviscid" nature of the asymmetry is demonstrated using the example of the separating unsteady flow of an ideal incompressible fluid around a cylinder which is expanding at a constant velocity, that is, a non-steady-state analogue of steady-state flow around a cone at an angle of attack. An asymmetric flow structure is realized for a symmetrical positioning of the points of separation of the vortex sheets. This is evidence of the secondary role of viscosity, which can manifest itself through an "inverse" effect on the position of the points of separation. New asymmetric solutions and processes by which they arise, which are different from the classical bifurcation of the symmetric solution, are found. Together with an investigation of stability, an analysis of the global pattern of "self-similar" streamlines is carried out in the selection of the "realizable" solutions. The global pattern must correspond to the scheme adopted when constructing the theoretical model.

The breakdown of the symmetry of separating flow around symmetric bodies (circular cones, combinations of a cone and a delta wing, a cone and a cylinder, etc.), which is well known from experiment [1], has been confirmed in recent years by numerical integration of the Navier–Stokes and Reynolds equations (for example, see [2–4]). Here, the possibility, in the case of laminar conditions, of achieving agreement between the experimental and calculated results, which is as close as may be desired, does not give rise to any doubt. In the case of turbulent conditions, the difference between the results is solely due to the non-universality of the models of turbulence used in the calculations. The development of these models will lead to a reduction in the disagreement between the results of calculation and experiment. On the other hand, the numerical modelling of an asymmetric viscous flow around symmetric bodies, which is as accurate as may be desired with the undoubted practical importance of the results which are obtained (especially, the force characteristics), while not revealing the cause of the onset of asymmetry, does create the impression that it is exclusively of a "viscous nature". In fact, this is not so as, in analogous problems of unsteady separating flow around expanding symmetric bodies, asymmetry arises in the ideal fluid model [5–7].

1. FORMULATION OF THE PROBLEM AND BASIC EQUATIONS

Suppose that a plane-parallel stream of an ideal fluid, which is uniform at infinity, flows around a circular cylinder which is expanding from the origin of the Cartesian coordinates xy at a velocity U = const (Fig. 1). The velocity vector of the free stream $\mathbf{V}_\infty$ is directed along the y axis.

As in [5], we shall model the separated flow around the cylinder using vortex sheets, which leave its surface from the points S_1 and S_2, symmetrically arranged with respect to the y axis with coordinates $z_{s1} = Re^{i\theta_1}$ and $z_{s2} = Re^{i\theta_2}$, where $R = Ut$ and $\theta_2 = \pi - \theta_1$. In turn, we shall model a vortex sheet with a vortex cut.

On changing from a vortex sheet to a vortex cut, the vorticity (the remainder of the velocity component which is tangential to the vortex sheet) "contracts" from the sheet into its "centre", which is transformed into a point vortex (more briefly, into a vortex) of finite intensity $\Gamma = \Gamma(t)$. Two forces appear on account of this. First, a Zhukovskii force $\mathbf{F}_1$ which is proportional to the product of Γ and the velocity of the vortex relative to the flow, that is, the difference $\mathbf{V}_k - dz_k/dt$, where $z_k = x_k + iy_k$ is the complex coordinate of the kth vortex (k = 1, 2) and $\mathbf{V}_k$ is the velocity of the flow when $z = z_k$ without the contribution from this vortex. Second, a force $\mathbf{F}_2$ which is due to the pressure drop which, in the case of such a transition, acts on the "trace" of the sheet, which is devoid of vorticity [8–12]. The pressure drop, which is proportional to $d\Gamma/dt$, depends solely on time. In the calculation of $\mathbf{F}_2$, this enables one to replace the trace of the sheet, which is unknown in advance, by a rectilinear cut which joins the point of separation

†*Prikl. Mat. Mekh.* Vol. 63, No. 1, pp. 63–70, 1999.

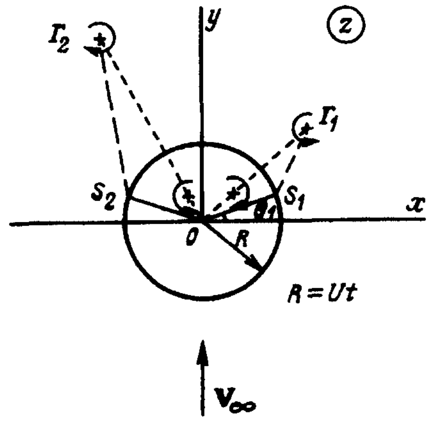

Fig. 1.

of the sheet with the point vortex. No forces of any kind act on the initial sheet. Hence, according to the recommendations in [8, 9], the equation of motion of the vortex is obtained by equating the sum $\mathbf{F}_1 + \mathbf{F}_2$ to zero. This gives the equation

$$\frac{dz_k^*}{dt} = \mathbf{V}_k^* + \frac{(z_{sk}^* - z_k^*)}{\Gamma_k} \frac{d\Gamma_k}{dt} \tag{1.1}$$

Henceforth, an asterisk denotes complex conjugation, $\mathbf{V}_k + u_k + i\upsilon_k$ is the velocity of the fluid at the point of location of the kth vortex (after subtracting the velocity which it induces itself), z_{sk} is the coordinate of the separation point to which the kth vortex is bound and $\Gamma_k(t)$ is its vorticity ($k = 1, 2$). We now change to the self-similar variables ζ_k and γ_k in accordance with the equations $z_k = \zeta_k R(t)$ and $\Gamma_k = 2\pi R(t)U\gamma_k$. In these variables, Eq. (1.1) becomes

$$\frac{d\zeta_k^*}{d\tau} - \frac{e^{-i\theta_k} - \zeta_k^*}{\gamma_k} \frac{d\gamma_k}{d\tau} = \frac{u_k - i\upsilon_k}{U} - 2\zeta_k^* + e^{-i\theta_k} \tag{1.2}$$

where $\tau = \ln t$ and $z_{sk} = Re^{i\theta_k}$.

In order to find u_k and υ_k, we construct a complex potential w, taking account of the vortices, which are "conjugated" with respect to the cylinder, at the points R^2/z_1^* and R^2/z_2^*, which is necessary in order to satisfy the slip conditions on the cylinder [5]

$$w = -iV_\infty\left(z - \frac{R^2}{z}\right) + UR\ln z + \frac{\Gamma_1}{2\pi i}\ln\frac{z - z_1}{z - R^2/z_1^*} - \frac{\Gamma_2}{2\pi i}\ln\frac{z - z_2}{z - R^2/z_2^*} \tag{1.3}$$

Here, the first three terms represent the sum of the complex potentials of the uniform free stream, the dipole and the source. The dipole and the source are located at the origin of the coordinate system, that is, at the centre of the cylinder. In accordance with what has been said previously

$$u_k - i\upsilon_k = \lim_{z \to z_k}\left(\frac{dw}{dz} - \frac{\Gamma_k}{2\pi i(z - z_k)}\right), \quad k = 1,\ 2$$

The slip velocity at the point $z = Re^{i\theta}$ on the cylinder is the imaginary part of $e^{i\theta}(i\upsilon - u)$. Hence, the condition for vortex sheets separating from two points on a cylinder, which states that the slip velocity is equal to zero at these points, has the form ($\alpha = V_\infty/U$)

$$\frac{(\zeta_1\zeta_1^* - 1)\gamma_1}{(e^{i\theta_k} - \zeta_1)(e^{-i\theta_k} - \zeta_1^*)} - \frac{(\zeta_2\zeta_2^* - 1)\gamma_2}{(e^{i\theta_k} - \zeta_2)(e^{-i\theta_k} - \zeta_2^*)} = 2\alpha\cos\theta_k, \quad k = 1,\ 2 \tag{1.4}$$

From these equations, the γ_k are expressed in terms of $\zeta_j = \xi_j + i\eta_j$ ($k, j = 1, 2$). We now introduce the four-dimensional vector $\mathbf{X} = (X_1, X_2, X_3, X_4) \equiv (\xi_1, \eta_1, \xi_2, \eta_2)$. Allowing for the fact that

$$\frac{d\gamma_k}{d\tau} = \sum_{m=1}^{4} \frac{\partial\gamma_k}{\partial X_m} \frac{dX_m}{d\tau}$$

we then write Eq. (1.2) in the form

$$(E + A)d\mathbf{X}/d\tau = \mathbf{F} \tag{1.5}$$

where E is a 4×4 identity and the elements A_{mn} of the matrix A and the components F_m of the vector **F** are defined by the formula

$$A_{1n} + iA_{2n} = \frac{X_1 + iX_2 - e^{i\theta_1}}{\gamma_1} \frac{\partial\gamma_1}{\partial X_n}, \quad A_{3n} + iA_{4n} = \frac{X_3 + iX_4 - e^{i\theta_2}}{\gamma_2} \frac{\partial\gamma_2}{\partial X_n}$$

$$F_1 + iF_2 = \frac{u_1 + iv_1}{U} - 2(X_1 + iX_2)e^{i\theta_1}, \quad F_3 + iF_4 = \frac{u_2 + iv_2}{U} - 2(X_3 + iX_4)e^{i\theta_2}$$

The self-similar solution of system (1.5) is independent of t or τ and, consequently, satisfies the "steady-state" equation $\mathbf{F}(\mathbf{X}) = 0$. After the solution of this equation has been found for some value of $\alpha = V_\infty/U$, the solutions for other α were constructed numerically by the method of continuation with respect to a parameter [13].

To investigate the stability of the self-similar solutions of system (1.5), we replaced it with the equivalent form

$$d\mathbf{X}/d\tau = (E + A)^{-1}\mathbf{F}$$

and linearized it in the neighbourhood of the stationary point $\mathbf{X}_0$, by representing $\mathbf{X}$ in the form $\mathbf{X} = \mathbf{X}_0 + \mathbf{X}^\circ$ with a small addition $\mathbf{X}^\circ$ such that $|\mathbf{X}^\circ| \ll |\mathbf{X}_0|$. We obtain

$$d\mathbf{X}^\circ/d\tau = (E + A)_0^{-1} J_0 \mathbf{X}^\circ \tag{1.6}$$

Here, $J \equiv \partial F/\partial X$ is the functional Jacobi matrix of the right-hand side of system (1.2). The zero subscript on the matrix and $(E + A)^{-1}$ denotes that they are calculated for $\mathbf{X} = \mathbf{X}_0$.

The solution of the linear system of ordinary differential equations (1.6), as usual, is sought in the form

$$\mathbf{X}^\circ = \sum_{i=1}^{4} C_i \mathbf{X}_i^\circ e^{\lambda_i \tau}$$

where C_i are arbitrary constants, λ_i are the eigenvalues of the matrix $(E + A)_0^{-1}J_0$, and $\mathbf{X}_i^\circ$ are the eigenvectors corresponding to them.

Note that the authors of [7] only speak of the eigenvalues of the matrix J_0 and make no mention of the matrix $(E + A)_0^{-1}$. This poses the question as to whether the results in [7] concerning the investigation of stability are correct. This primarily concerns the simultaneous existence (for the same value of α) of the symmetric and asymmetric stable solutions found in [7].

If the eigenvalue λ_i, which is a root of the characteristic equation, lies in the right half-plane ($\mathrm{Re}\, \lambda_i > 0$), we shall call such a root an unstable root. We shall distinguish unstable solutions using the number of unstable roots. When there is just one eigenvalue in the right half-plane, we shall say that the solution is simply "unstable" and, when there are two, "doubly unstable" and so on.

2. DISCUSSION OF THE RESULTS

In [5–7], the transition from the symmetric solution to an asymmetric solution was the result of a bifurcation of the symmetric solution at a certain value of the parameter $\alpha = \alpha_*$. A unique symmetric solution exists when $\alpha < \alpha_*$. Being stable everywhere, with the exception of a small neighbourhood of the point a, which we shall discuss below, it becomes unstable when $\alpha > \alpha_*$. A stable asymmetric solution simultaneously appears. Such a situation is illustrated in Fig. 2, in which the ordinates of the vortices η_i are given as functions of the parameter α at the fixed points of separation $\theta_1 = 45°$ and $\theta_2 = 135°$. The part of the symmetric solution ab is stable while the part bc is unstable. On the curve ac $\eta_1 = \eta_2$

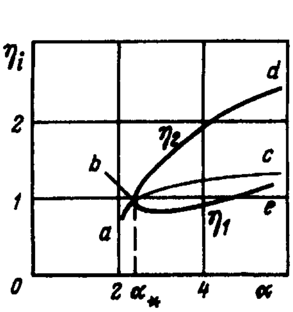

Fig. 2.

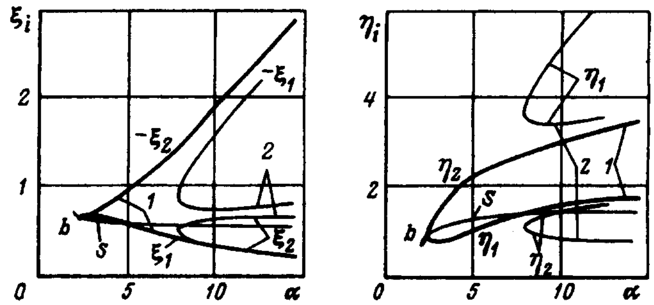

Fig. 3.

by virtue of symmetry. A second, asymmetric solution (curves *be* and *bd* for η_1 and η_2, respectively), which is stable when $\alpha > \alpha_*$, appears at the point of bifurcation *b*. Stable (unstable) solutions are given by the solid (thin) curves in Fig. 2 and later figures.

A more detailed numerical analysis of the system of equations (1.4)–(1.6) with the same position of the separation points showed that a further two asymmetric solutions exist for large values of α. They are indicated with the number 2 in Fig. 3. One of these is unstable and the other is doubly unstable. Furthermore, these solutions contradict the physical formulation of the problem and must be discarded for the reason explained below in the case of another position of the separation points.

There is no bifurcation point at separation angles of the sheets of $\theta_1 = 35°$ and $\theta_2 = 145°$. In this case (Fig. 4), the symmetric solution, which is denoted by the letter *S*, is unstable and the asymmetric solution, indicated with the number 1, is stable for all values of the parameter α. This solution appears at a certain $\alpha > \alpha_m$. For smaller values of α there is no asymmetric solution corresponding to the arrangement of vortex cuts which has been adopted and the symmetric solution is unstable. Consequently, solutions with a self-similar dependence of the parameters on time do not exist within the framework of the model which has been adopted with the chosen symmetric arrangement of the points where the sheets leave ("points of separation"). Using the well-known methods of prevention and organization of separation, a similar situation can also be expected in steady-state flows of a real (viscous) gas or liquid and the unsteady problem being considered serves as an analogue of such flows.

As in the preceding example, there are two non-physical solutions, indicated with the number 2, when $\theta_1 = 35°$ and $\theta_2 = 145°$. One of these solutions is unstable and the other is doubly unstable. The streamlines of one of them (the unstable one) for $\alpha = 12.27$ are plotted in Fig. 5. In this example, the coordinates of the vortices are equal to $\xi_1 = -1.96$, $\eta_1 = 3.88$, $\xi_2 = 0.53$ and $\eta_2 = 1.57$. Henceforth, the trajectories of particles written in self-similar variables are called streamlines. In the initial variables, they are determined by the differential equation $dz/dt = \mathbf{V} = u + i\upsilon$ in accordance with the definition. After changing to the self-similar variables ξ and η, we obtain from this that

$$\frac{d\xi}{d\eta} = \frac{u/U - \xi}{\upsilon/U - \eta} \tag{2.1}$$

In the determination of the velocity components u and υ as functions of ξ and η, it is convenient to use the complex potential $w^\circ = w^\circ(\zeta) = w(Ut\zeta, Ut, 2\pi U^2 t\gamma_{1,2})/(Ut)$ instead of the complex potential

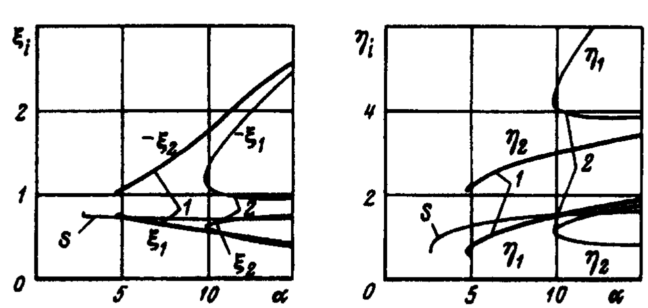

Fig. 4.

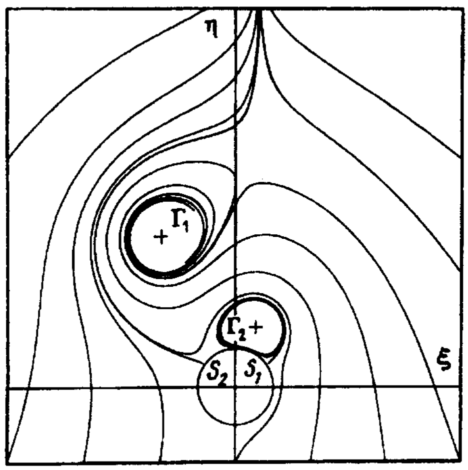

Fig. 5.

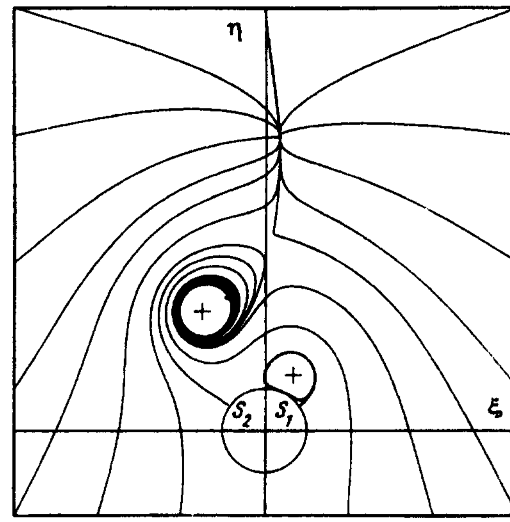

Fig. 6.

$w = w(z, R, \Gamma_{1,2})$ and the formula $dw^\circ/d\zeta = u - i\upsilon$. In accordance with (1.3), this gives

$$w^\circ = -iV_\infty\left(\zeta - \frac{1}{\zeta}\right) + U\left(\ln\zeta + \frac{\gamma_1}{i}\ln\frac{\zeta-\zeta_1}{\zeta-1/\zeta_1^*} - \frac{\gamma_2}{i}\ln\frac{\zeta-\zeta_2}{\zeta-1/\zeta_2^*}\right)$$

$$u - iv = -iV_\infty\left(1 + \frac{1}{\zeta^2}\right) + U\left[\frac{1}{\zeta} + \frac{\gamma_1}{i}\left(\frac{1}{\zeta-\zeta_1} - \frac{1}{\zeta-1/\zeta_1^*}\right) - \frac{\gamma_2}{i}\left(\frac{1}{\zeta-\zeta_2} - \frac{1}{\zeta-1/\zeta_2^*}\right)\right] \tag{2.2}$$

The streamlines are obtained as a result of the numerical integration of Eq. (2.1) with u and υ from (2.2) for an arbitrary choice of the starting point in the plane of the self-similar variables. As applied to steady three-dimensional flow around a cone at an angle of attack, they give the pattern of intersections of the conical flow surfaces with an arbitrary plane (by virtue of the self-similarity of the solution) perpendicular to the axis of the cone.

It can be seen from the streamlines, which were calculated using the method described above and are shown in Fig. 5, that the vortex which is "attached" through its equation of motion to the right separation point S_1 is found in the left half-plane (the coordinate ξ_1 is negative), while the vortex "attached" to the left point S_2 is in the right half-plane. This, however, does not correspond to the initial formulation of the problem. Actually, the streamline which is a trace of a vortex sheet and emerges from the point S_1, winds round the right rather than the left vortex. The streamline emerging from the point S_2 departs to infinity and is not associated with any vortex.

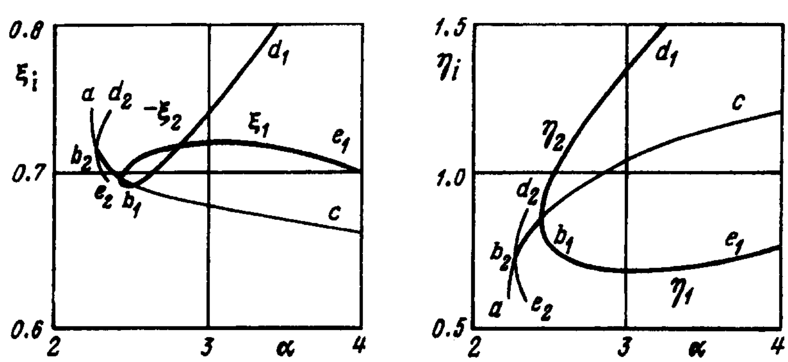

Fig. 7.

The streamline pattern for the physical solution, indicated with the number 1 in Fig. 4, is given for comparison in Fig. 6 for the case when $\alpha = 7.93$. In this example, $\xi_1 = 0.68$, $\eta_1 = 1.32$, $\xi_2 = -1.48$ and $\eta_2 = 2.82$. Here, the traces of the vortex sheets are wound on "their own" vortices.

Figure 5 shows that system (1.4)–(1.6) admits of extremely exotic solutions, the non-physical nature of which follows from an analysis of the global flow pattern. In such situations, the method of selecting solutions proposed in [5], which reduces to an analysis of the behaviour of the velocity on the cylinder surface at the points of separation of the sheets with the object of finding whether they are not stagnation points, is insufficient.

It has been noted earlier that the bifurcation of the solution disappears (see Figs 4 and 5) when the angular coordinate of the separation of the vortex sheet θ_1 is reduced from 45° to 35°. This disappearance is accompanied by the appearance of yet another bifurcation point b_2 at a certain intermediate value of θ_1. For instance, when $\theta_1 = 42°$ (see Fig. 7), together with the previous bifurcation point b_1 and the asymmetric solution branch $d_1b_1e_1$, there is a second bifurcation point b_2 with an asymmetric solution branch $d_2b_2e_2$ corresponding to it. As a stability analysis showed, the last-mentioned, as well as the segments ab_2 and b_1c of the symmetric solution, are unstable, in complete agreement with [14] (see §II 10). The remaining branches, b_1b_2 and $d_1b_1e_1$, correspond to the symmetric and asymmetric stable solutions, respectively.

Note that the assertion in [15], that the minimum value of the parameter α for which a symmetric solution exists is equal to $\alpha_0 = 1.5/\sin\theta$, is incorrect. The branch of the symmetric solution in the case when $\theta_1 = 35°$ is drawn in Fig. 8 on a larger scale than in Fig. 4. The solution with the vortices located directly on the cylinder surface corresponds to point a. In fact, in it $\alpha = \alpha_0$. However, the minimum value of $\alpha = \alpha_m$ is reached at point m when the vortices are located at a small distance from the cylinder surface. There are two solutions in the range $\alpha_m < \alpha < \alpha_0$. For one of them, am, the number of unstable roots is greater by one than for the other, mc. The situation which has been described is typical of small neighbourhoods of the "left end" points of the curves corresponding to both symmetric and asymmetric solutions. In the case of the asymmetric solutions, this occurs when, as in the case shown in Fig. 4, they do not appear as the result of a bifurcation of the symmetric solution.

In concluding, we shall dwell in more detail on what appears to us to be two rather important features. We begin with the "key" role of the transition from vortex sheets, that is, from tangential discontinuities, to vortex cuts. At first glance, "the baby is thrown out with the bath water" in such a transition. However, tangential discontinuities are unstable and getting rid of them removes from the initial model the mechanism for the onset of instability, which is always inherent in it. As a matter of fact, the above-mentioned operation not only does not hinder our understanding of the nature of the onset of asymmetry in the flows under investigation but, on the contrary, helps this. Actually, turbulent mixing zones are formed in place of the tangential discontinuities as a result of their instability. Such "stable-on-average" zones will exist both in the case of a symmetric and an asymmetric flow around a body. Hence, the above-mentioned instability, while affecting the "transitional" value of the parameter α at which the symmetric solution becomes unstable (or vice versa), can hardly play the role of a mechanism for the onset of asymmetry.

Similar considerations also hold with respect to the inverse effect of flow asymmetry which has arisen on the necessarily asymmetric position, associated with the separation of the boundary layer, of the

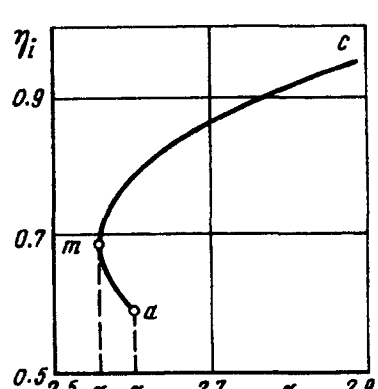

Fig. 8.

points of separation of the sheets, which more accurately correspond to mixing zones. Moreover, in principle, it is possible to develop a method to take account of the above-mentioned viscous effects. However, the aim of this paper was not to create a method as an alternative to direct numerical modelling of such flows but to demonstrate the inviscid nature of their asymmetry. In view of this, the symmetrical arrangement of the points of separation of the sheets is actually justified. Furthermore, the analysis which has been carried out under the assumption that the points of separation of the sheets are symmetrically arranged is of interest not only theoretically but, also, for applications. Actually, the methods of boundary-layer control which are available to workers, e.g. blowing and the setting up of special shields, "interceptors" on the body, enable one both to delay as well as to initiate its separation. Early separation leads to an increase in drag while an asymmetric flow leads to the appearance of lateral forces which act on the flying object. Since both of these results are generally undesirable, it is natural to strive, first, to delay separation for as long as possible and, second, when there is no knowledge regarding the cause of the asymmetry, to make it symmetric. It is seen from a comparison of Figs 3 and 4 that the "transitional" value of the parameter α, which is an analogue of the angle of attack in the case of steady flow around conical bodies, decreases in this case. Consequently, in spite of the expectations of workers, undesirable lateral forces arise at lower angles of attack than in the case of earlier separation of the boundary layer.

It follows from the above analysis and the preceding explanations that the behaviour of the "vortex nuclei" play a fundamental role in the realization of symmetric or asymmetric flow around a body. In the ideal fluid approximation, these are spiral-like formations on which the vortex sheet is wound an infinite number of times. The pressure is negative in the neighbourhood of their "centre". In the inviscid approximation, taking account of compressibility, which excludes negative pressures, leads to the winding of a sheet on a "vacuum nucleus" of finite radius. It is natural that, as a result of the effect of viscosity, such non-physical formations are replaced with "viscous nuclei" with a lower but positive pressure and with rotation of the gas or liquid particles according to a law which is close to the law of rotation for a solid (For example, see [16]). However, in spite of the strong effect of viscosity in the nucleus of a vortex, its action on the remaining practically inviscid flow is equivalent to the action of a point vortex, which is introduced as was done above. By the way, we recall that, in algorithms which assume the construction of a sheet in the ideal fluid model, only one to two of the loops are constructed, using special measures which "stabilize" the sheet, and the rest of it is replaced with a vortex cut as was done above [11].

All calculations were carried out using the REDUCE analytical computational system.

We wish to thank V. I. Kopchenov and K. E. Lomkov for their participation in the initial stage of this research and A. G. Kulikovskii for useful remarks.

This research was supported financially by the Russian Foundation for Basic Research (96-01-01825 and 96-15-96158).

REFERENCES

1. ERICSSON, L. E., Thoughts on conical flow asymmetry. *AIAA Jnl*, 1993, **31**, 1563–1568.
2. LEVY, Y., HESSELINK, L. and DEGANI, D., Anomalous asymmetries in flows generated by algorithms that fail to conserve symmetry. *AIAA Jnl*, 1995, **33**, 999–1007.
3. DUSING, D. W. and ORKWIS, P. D., Numerical issues affecting vortex asymmetries computed with the conical Navier–Stokes equations. *Computers and Fluids*, 1996, **25**, 319–334.
4. HWANG, S. J. and RHO, O. H., Lower-upper symmetric Gauss–Seidel scheme exhibiting asymmetric vortices over slender bodies. *J. Spacecraft and Rockets*, 1996, **33**,750–752.
5. DYER, D. E., FIDDES, S. P. and SMITH, J. H. B., Asymmetric vortex formation from cones at incidence—a simple inviscid model. *Aeronaut. Quart.*, 1982, **33**, 293–312.
6. GOMAN, M. G. and KHRABROV, A. N., The onset of asymmetric separated flow around thin solids of revolution at high angles of attack. *Uch. Zap. TsAGI*, 1984, **15**, 6, 1–9.
7. GOMAN, M. G., ZAKHAROV, S. B. and KHRABROV, A. N., Symmetric and asymmetric separated flow around a low-aspect-ratio wing with a fuselage. *Uch. Zap. TsAGI*, 1985, **16**, 6, 1–8.
8. EDWARDS, R. H., Leading-edge separation from delta wings. *J. Aeronaut. Sci.*, 1954, **21**, 134–135.
9. BROWN, C. E., MICHAEL, W. H., Jr, Effect of leading-edge separation on the lift of a delta wing. *J. Aeronaut. Sci.*, 1954, **21**, 690–694, 706.
10. KOPCHENOV, V. I., KRAIKO, A. N. and LOMKOV, K. E., The modelling of a separated flow of an ideal incompressible fluid around a plate of finite width. In *Aerodynamics*. Izd. Saratov. Unov., Saratov, No. 11(14), 8–23, 1988.
11. KOPCHENOV, V. I., KRAIKO, A. N. and SHCHIPIN, S. K., The self-similar problem of the separated flow of an ideal fluid around an expanding plate. *Izv. Akad. Nauk SSSR. MZhG*, 1988, 5, 62–69.
12. KOPCHENOV, V. I., KRAIKO, A. N. and LOMKOV, K. E., Unsteady separated flow of an ideal incompressible fluid around an instantaneously accelerated plate of finite width. *Uch. Zap. TsAGI*, 1997, **28**, 53–64.
13. GOMAN, M. G., A differential method for the continuation of the solutions of systems of finite non-linear equations depending on a parameter, *Uch. Zap. TsAGI*, 1986, **17**, 5, 94–102.

14. IOSS, G. and JOSEPH, D., *Elementary Stability and Bifurcation Theory*. Springer, New York, 1980.
15. BRYSON, A. E., Symmetric vortex separation on circular cylinders and cones. *Trans. ASME. Ser. E.J. Appl. Mech.*, 1959, **26**, 643–648.
16. TRIGUB, V. N., BLOKHIN, A. B. and SIMAKIN, I. N., The asymptotic study of dissipation and breakdown of a wing-tip vortex. *J. Fluid Mech.*, 1994, **274**, 293–337.

Translated by E.L.S.